Supplementary Information: Raman spectroscopy of GaSe and InSe post-transition metal chalcogenides layers

Maciej R. Molas,[1] Anastasia V. Tyurnina,[2,3,4] Viktor Zólyomi,[2,3] Anna Ott,[5] Daniel J. Terry,[2,3] Matthew Hamer,[2,3] Celal Yelgel,[3] Albert G. Nasibulin,[4] Andrea C. Ferrari,[5] Vladimir I. Fal'ko,[2,3,6] and Roman V. Gorbachev[2,3,6]

[1] *Institute of Experimental Physics, Faculty of Physics, University of Warsaw, ul. Pasteura 5, 02-093 Warszawa, Poland*
[2] *School of Physics and Astronomy, University of Manchester, Oxford Road, M13 9PL, UK*
[3] *National Graphene Institute, University of Manchester, Booth St E, Manchester M13 9PL, UK*
[4] *Skolkovo Institute of Science and Technology, Nobel St. 3, 143026 Moscow, Russia*
[5] *Cambridge Graphene Centre, University of Cambridge, 9 JJ Thomson Avenue, Cambridge CB3 0FA, UK*
[6] *Henry Royce Institute, University of Manchester, Oxford Road, Manchester, M13 9PL, UK*

S1. SELECTION RULES FOR E′ AND E″ PHONONS

To understand the selection rules for E′ and E″ phonons in InSe and GaSe, we construct an invariant that respects the threefold rotational symmetry common to all N. We restrict ourselves to vertical incidence of light, where polarization is in-plane, consistent with our measurements.

Let us denote the electric field vector of the incoming and outgoing photon by $\mathbf{E_1}$ and $\mathbf{E_2}$, respectively, and the phonon displacement vector as $\mathbf{u}$. Taking angular momentum conservation into account, an invariant with respect to threefold in-plane rotation can be defined as:

$$\begin{aligned} I = &\alpha(E_{1x}+iE_{1y})(u_x+iu_y)(E_{2x}+iE_{2y}) \\ &+\alpha^*(E_{1x}-iE_{1y})(u_x-iu_y)(E_{2x}-iE_{2y}), \end{aligned} \quad (1)$$

where $\alpha=\alpha'+i\alpha''$ is a complex prefactor which depends on how close the exciting laser energy is to resonance. The invariant can be simplified to:

$$\begin{aligned} I = &\alpha'(E_{1x}u_xE_{2x}-E_{1x}u_yE_{2y}-E_{1y}u_xE_{2y}-E_{1y}u_yE_{2x}) \\ &+\alpha''(E_{1y}u_yE_{2y}-E_{1y}u_xE_{2x}-E_{1x}u_yE_{2x}-E_{1x}u_xE_{2y}), \end{aligned} \quad (2)$$

which can be grouped into terms proportional to u_x and u_y as:

$$\begin{aligned} I = &u_x(\alpha'E_{1x}E_{2x}-\alpha'E_{1y}E_{2y}-\alpha''E_{1x}E_{2y}-\alpha''E_{1y}E_{2x}) \\ &+u_y(\alpha'E_{1x}E_{2x}-\alpha'E_{1y}E_{2y}-\alpha''E_{1x}E_{2y}-\alpha''E_{1y}E_{2x}), \end{aligned} \quad (3)$$

In matrix form, we can write this as:

$$I = u_x\mathbf{E_1^T}\begin{pmatrix}\alpha' & -\alpha''\\ -\alpha'' & -\alpha'\end{pmatrix}\mathbf{E_2}+u_x\mathbf{E_1^T}\begin{pmatrix}-\alpha'' & -\alpha'\\ -\alpha' & \alpha''\end{pmatrix}\mathbf{E_2}, \quad (4)$$

α', α'' determine the scattering probabilities as follows. For parallel ($\mathbf{E_1} \parallel \mathbf{E_2}$) polarizations, the scattering probability of u_x and u_y phonons is α'^2 and α''^2, respectively, which sum up to $\alpha'^2+\alpha''^2 \equiv |\alpha|^2$. For perpendicular ($\mathbf{E_1} \perp \mathbf{E_2}$) polarizations, the scattering probability of u_x and u_y phonons is α''^2 and α'^2, respectively, which sum up to $\alpha'^2+\alpha''^2 \equiv |\alpha|^2$, the same as the parallel configuration. Therefore, E′ and E″ phonons give the same Raman response in all polarization configurations.

TABLE S1. Γ-point phonons for 1L-GaSe (ω_{GaSe}) and InSe (ω_{InSe}) from DFT (LDA using the VASP code). The first column shows the symmetry classification according to the D_{3h} point group (Irrep.). In the last column, we show the parallel:crossed polarization intensity ratios. 0:0 means that the mode is Raman inactive.

Irrep.	ω_{GaSe} (cm^{-1})	ω_{InSe} (cm^{-1})	Int. ratio
E″	55.4	36.7	1:1
A_1'	129.8	109.6	1:0
E″	211.6	175.7	1:1
E′	217.0	179.7	1:1
A_2''	248.3	203.1	0:0
A_1'	312.5	232.4	1:0

The above findings are universally applicable to InSe, GaSe of any N, and other hexagonal PTMCs, as they are a consequence of the threefold C_3 rotational symmetry, which is always present in these materials regardless of N or stacking order.

To verify the above analysis, we used first principles DFT in the local density approximation (LDA) using the VASP code[1] to calculate the Raman tensors. TableS1, summarizes the phonon frequencies of 1L-InSe and GaSe at the Γ-point. The in-plane phonon modes, i.e. E′ and E″, are active in both polarizations: parallel and crossed, indicated by 1:1. At the same time, the A_1' modes are observable only for parallel polarization c(1:0), since these are non-degenerate.

Note that the A_2'' mode is inactive (0:0) due to the $z \to -z$ reflection symmetry in 1L. This becomes active in MLs, where the reflection symmetry is broken, and the intensity ratio becomes 1:0. The observation of this mode in the Raman spectrum of 1L-InSe may be due to symmetry breaking caused by interaction with the hBN encapsulant, but the same does not happen in 1L-GaSe.

S2. Γ-POINT FREQUENCIES IN FL-GASE AND INSE

In order to study N dependence of the phonon frequencies GaSe and InSe, we carry out DFT calculations using Quantum Espresso[2] (QE) to calculate the frequencies of 1L, 2L and 3L GaSe and InSe. We use ε-stacking for GaSe and γ-stacking for InSe. TablesS2,S3, S4 compare theory to experiments.

TABLE S2. Γ-point phonon frequencies in cm^{-1} for 1L-GaSe ($\omega_{\rm GaSe}$) and InSe ($\omega_{\rm InSe}$) according to DFT (LDA using Quantum Espresso). The first column shows the symmetry classification according to the D_{3h} point group (Irrep.). The fourth column gives then parallel:crossed polarization intensity ratios. 0:0 ratio means that the mode is Raman inactive. The measured values ($\omega^{exp}_{\rm GaSe}$ and $\omega^{exp}_{\rm InSe}$), discussed in the main text, are also shown

Irrep.	$\omega^{LDA}_{\rm GaSe}$	$\omega^{LDA}_{\rm InSe}$	Int. ratio	$\omega^{exp}_{\rm GaSe}$	$\omega^{exp}_{\rm InSe}$
E″	59.9	41.3	1:1		
A_1'	130.6	110.9	1:0	132.8	114.9
E″	211.1	175.0	1:1	214.4	180.1
E′	216.1	178.7	1:1		
A_2''	252.0	206.6	0:0		202.4
A_1'	316.4	237.5	1:0	309.2	228.6

For 1L-GaSe and InSe, we compare the calculated frequencies obtained using VASP, Table S1, and using QE, Table S2. The QE predictions deviate from the VASP data by up to $5cm^{-1}$. This is due to using different pseudopotentials and approaches in the two codes (density functional perturbation theory in QE, and finite differences approximation with 4×4 supercells in VASP). The computed phonon frequencies are in good agreement with the measured data, with a maximum deviation$\sim9cm^{-1}$.

For 2L, 3L, the phonon modes are subject to Davydov splitting[3] caused by the interaction between the layers. Each layer mode splits into a number of modes equal to the total N, i.e. 2 in 2L, 3 in 3L, Tables S3, S4. However, due to the weak nature of the inter-layer interaction, the Davydov splitting is very small$\sim1cm^{-1}$, and not resolved in our measurements. This Davydov splitting has been detected in TMDS, e.g. WS_2[4] and $MoTe_2$[5,6], where it was found that the detection of Davydov splitting depends strongly on the excitation energy: the splitting was not observed in the case of non-resonant excitation, while it was seen under resonant excitation. The absence of Davydov splitting in our measurements may be caused by the non-resonant excitation used in our experiments, combined with the small magnitude of the theoretically predicted splitting.

TABLE S3. Γ-point phonon frequencies in units of cm^{-1} for 2L-GaSe ($\omega_{\rm GaSe}$) and InSe ($\omega_{\rm InSe}$) according to DFT (LDA using the Quantum Espresso code). The first column shows the symmetry classification according to the C_{3v} point group (Irrep.). The fourth column reports the parallel:crossed polarization intensity ratios. The experimental phonon modes ($\omega^{exp}_{\rm GaSe}$ and $\omega^{exp}_{\rm InSe}$), discussed in the main text, are also shown

Irrep.	$\omega^{LDA}_{\rm GaSe}$	$\omega^{LDA}_{\rm InSe}$	Int. ratio	$\omega^{exp}_{\rm GaSe}$	$\omega^{exp}_{\rm InSe}$
E	19.4	12.7	1:1		
A_1	23.2	22.9	1:0		
E	58.5	41.5	1:1		
E	60.7	43.1	1:1		
A_1	130.3	109.4	1:0	134.4	115.1
A_1	131.5	112.5	1:0		
E	209.9	174.0	1:1	213.6	178.3
E	211.0	175.0	1:1		
E	215.4	177.5	1:1		
E	216.5	178.7	1:1		
A_1	250.4	204.6	1:0		201.3
A_1	251.2	205.8	1:0		
A_1	315.1	234.9	1:0	308.1	228.6
A_1	315.3	235.4	1:0		

TABLE S4. Γ-point phonon frequencies of 3L-ε-GaSe ($\omega_{\rm GaSe}$) and 3L-γ-InSe ($\omega_{\rm InSe}$) according to DFT (LDA using the Quantum Espresso code). The first three columns show the symmetry classification according to the D_{3h} point group (Irrep.), the frequency, and the parallel:crossed polarization intensity ratios, for 3L GaSe. The last three columns show the symmetry classification according to the C_{3v} point group (Irrep.), the frequency, and the parallel:crossed polarization intensity ratios, for 3L InSe. The 0:0 ratio means that the mode is Raman inactive. The experimental phonon modes ($\omega^{exp}_{\rm GaSe}$ and $\omega^{exp}_{\rm InSe}$) are also shown

Irrep.	$\omega^{LDA}_{\rm GaSe}$	Int. ratio	$\omega^{exp}_{\rm GaSe}$	Irrep.	$\omega^{LDA}_{\rm InSe}$	Int. ratio	$\omega^{exp}_{\rm InSe}$
E″	15.1	1:1		E	9.0	1:1	
A_1'	16.3	1:0		A_1	16.0	1:0	
E′	21.8	1:1		E	16.0	1:1	
A_2''	29.6	0:0		A_1	28.7	1:0	
E″	58.5	1:1	40.5	E	41.3	1:1	40.3
E′	59.5	1:1		E	42.4	1:1	
E″	62.0	1:1		E	43.5	1:1	
A_1'	130.4	1:0		A_1	109.3	1:0	
A_2''	131.8	0:0		A_1	110.9	1:0	
A_1'	133.3	1:0	134.6	A_1	113.6	1:0	115.7
E″	209.5	1:1		E	173.7	1:1	
E′	210.5	1:1		E	174.3	1:1	
E″	211.0	1:1	213.9	E	175.0	1:1	178.5
E′	214.7	1:1		E	177.3	1:1	
E″	216.1	1:1		E	178.2	1:1	
E′	216.4	1:1		E	178.7	1:1	
A_2''	249.5	0:0		A_1	203.2	1:0	200.8
A_2''	250.9	0:0		A_1	204.9	1:0	
A_1'	251.5	1:0		A_1	205.5	1:0	
A_1'	314.0	1:0	308.0	A_1	233.9	1:0	228.2
A_2''	315.1	0:0		A_1	234.7	1:0	
A_1'	315.2	1:0		A_1	235.1	1:0	

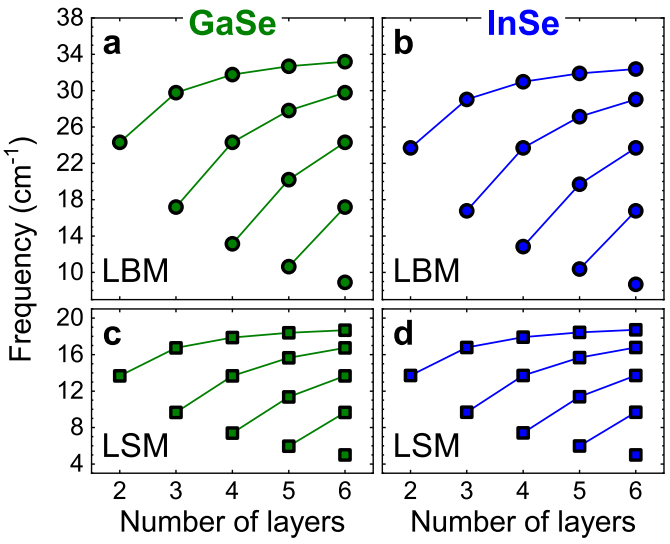

FIG. S1. N dependence of LBM and C frequencies from DFT for GaSe and InSe.

TABLE S5. Calculated LBM and C frequencies in units of cm^{-1} for N-layer GaSe and InSe. The measured C frequencies (ω^{exp}_{GaSe} and ω^{exp}_{InSe}) are also

N	ω^{LBM}_{GaSe}	ω^{C}_{GaSe}	ω^{exp}_{GaSe}	ω^{LBM}_{InSe}	ω^{C}_{InSe}	ω^{exp}_{InSe}
2	24.31	13.67	13.7	23.71	13.70	12.5
3	17.19	9.66	10.0	16.77	9.69	9.0
3	29.77	16.74	16.5	29.04	16.78	15.9
4	13.15	7.40	7.1	12.83	7.41	
4	24.31	13.67	13.3	23.71	13.70	
4	31.76	17.86	17.8	30.98	17.90	
5	10.62	5.97		10.36	5.99	
5	20.21	11.36		19.71	11.39	10.6
5	27.81	15.64		27.13	15.67	14.9
5	32.69	18.38		31.89	18.43	18.0
6	8.90	5.00		8.68	5.01	
6	17.19	9.66		16.77	9.69	
6	24.31	13.67		23.71	13.70	
6	29.77	16.74		29.04	16.78	
6	33.20	18.67		32.39	18.71	

We also calculated the LB and C modes in 2-6L GaSe and InSe, following the LCM and using DFT to calculate the force constants for the model. The calculated frequencies are summarized in Table S5 and visualized in Fig.S1, highlighting the evolution of multiple branches of modes as N increases. The LBM frequencies exhibit stronger dependence on N than the C frequencies: for 6L, the LBM changes from$\sim$9cm^{-1} to$\sim$33cm^{-1}, while C varies from$\sim$5cm^{-1} to$\sim$19cm^{-1}. The theoretically predicted C modes in good agreement with experiments, see Table S5.

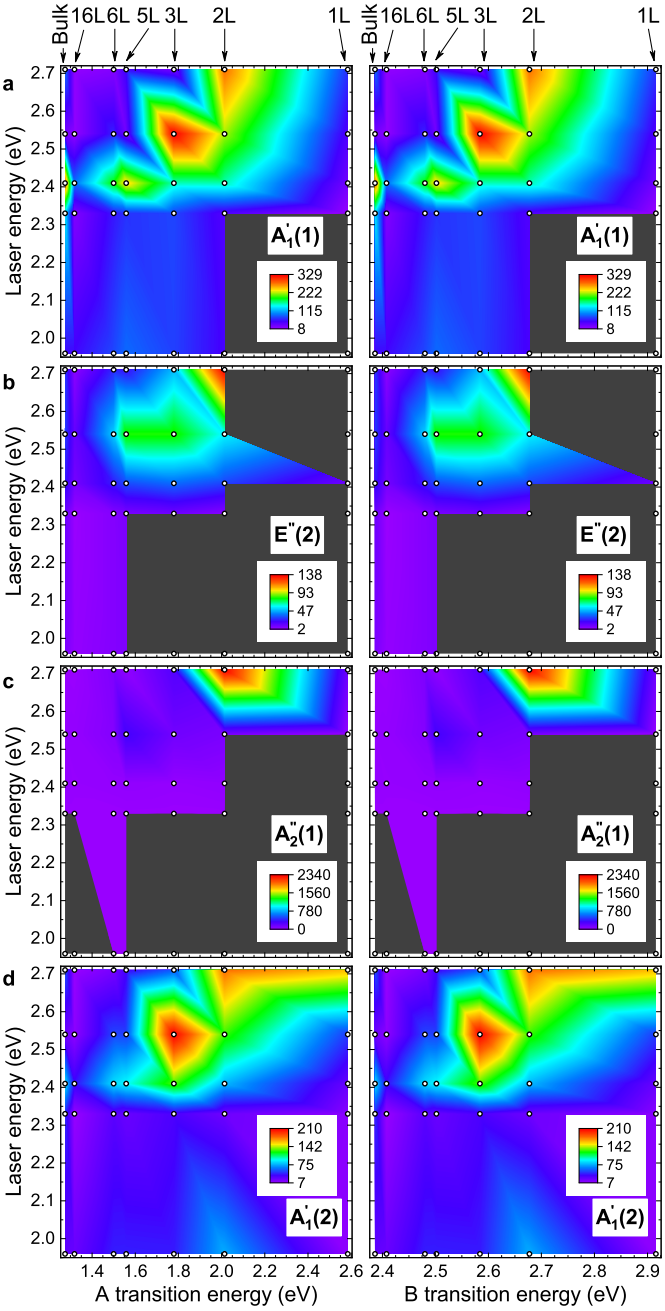

FIG. S2. Color-coded Raman intensity map of InSe layers as a function of excitation energy and (left panels) A and (right panels) B transition energies for various phonon modes: a $A_1^{'}(1)$, b $E^{"}(2)$, c $A_2^{"}(1)$, and d $A_1^{'}(2)$. The circle points represent the experimental data, while between them a linear extrapolation is implemented. The grey color corresponds to the energy range for which data are not extrapolated.

S3. RESONANCE EFFECTS

One of the substantial differences between the measured Raman spectra of GaSe and InSe layers is the variation of the intensity ratios between phonon modes for

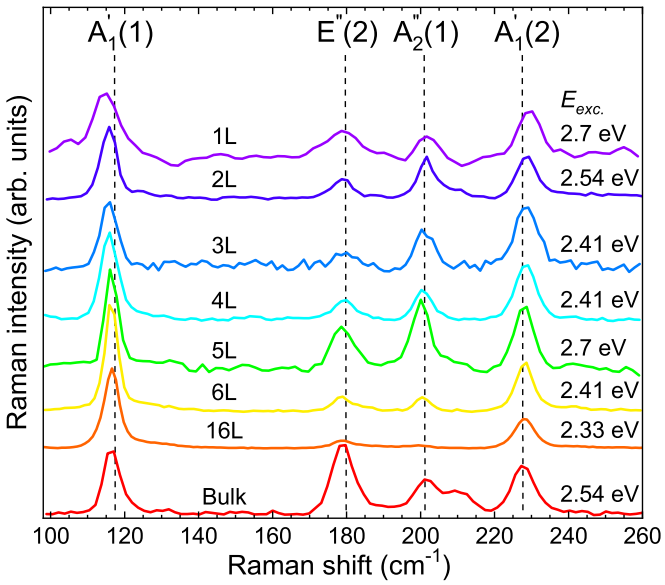

FIG. S3. Raman spectra for 1L to bulk InSe measured under various excitation energies ($E_{exc.}$). Dashed lines show peak positions for bulk.

InSe. The intensity of the $A_2^{"}(1)$ modes is significantly enhanced for 5L. This effect (enhancement of Raman lines and/or activation of additional phonon modes) is commonly reported for thin layers of S-TMDs[7–9]. A similar behavior was also observed for GaSe thin layers[10], where it was attributed to a resonance effect between optical band gap (photoluminescence) and laser excitation energy. To investigate the resonance influence, we perform an analysis of Raman spectra measured under a series of excitation energies, i.e. 1.96, 2.33, 2.41, 2.54,2.7eV. Fig.S2 plots a color-coded Raman intensity map as a function of excitation energy and the A,B transition energies for $A_1^{'}(1)$, $E^{"}(2)$, $A_2^{"}(1)$, $A_1^{'}(2)$. Depending on the experimental setup and N, the laser power and acquisitions setting are adjusted in order to obtain reasonable signal to noise ratio. All intensities in Fig.S2 are then normalized by N, laser power and acquisition time. In the case of InSe, there are two typically reported transitions: A and B. The first is related to the optical band gap (photoluminescence), while the second one is attributed to a high energy transition (hot luminescence)[11]. Both these transitions are affected by N. Their energies increase with decreasing N[11]. A comparison of A/B and excitation energies shows that the laser energies are close to B in most cases. In this case, the Raman signal is enhanced, as for right panel of Fig.S2a. In the case of $A_1^{'}(2)$, an increase of intensity is also observed at 1.96eV in 2L, which corresponds to resonance with A. However, this enhancement is much smaller than that with B. This may be related to the shape and the number of electronic levels in the conduction band 11.

Fig.S3 plots the Raman spectra for InSe flakes of varying N, measured with a laser excitation that avoids hot luminescence. The photoluminescence peaks are broader than the Raman peaks, therefore the mapped area around the maximum value of intensity is also broad.

[1] G. Kresse, J. Furthmuller, Phys. Rev. B **54**, 11169 (1996).
[2] P. Giannozzi et al. J. Phys. C **21**, 395502 (2009).
[3] A. S. Davydov, Soviet Physics Uspekhi **7**, 145 (1964).
[4] M. Staiger, R. Gillen, N. Scheuschner, O. Ochedowski, F. Kampmann, M. Schleberger, C. Thomsen, J. Maultzsch, Phys. Rev. B **91** (2015)
[5] G. Froehlicher, E. Lorchat, F. Fernique, C. Joshi, A. Molina-Sanchez, L. Wirtz, S. Berciaud, Nano Lett. **15**, 6481 (2015).
[6] M. Grzeszczyk, K. Golasa, M. Zinkiewicz, K. Nogajewski, M. R. Molas, M. Potemski, A. Wysmolek, A. Babinski, 2D Materials **3**, 025010 (2016).
[7] K. Golasa, M. Grzeszczyk, P. Leszczynski, C. Faugeras, A. A. L. Nicolet, A. Wysmolek, M. Potemski, A. Babinski, Appl. Phys. Let. **104**, 092106 (2014).
[8] M. Placidi, M. Dimitrievska, V. Izquierdo-Roca, X. Fontane, A. Castellanos-Gomez, A. Perez-Tomas,N. Mestres, M. Espindola-Rodriguez, S. Lopez-Marino, M. Neuschitzer, V. Bermudez, A. Yaremko, A. Perez-Rodrguez, 2D Materials **2**, 035006 (2015).
[9] M. Grzeszczyk, K. Golasa, M. R. Molas, K. Nogajewski, M. Zinkiewicz, M. Potemski, A. Wysmolek, A. Babinski, Scientific Reports **8** (2018).
[10] D. J. Terry, V. Zolyomi, M. Hamer, A. V. Tyurnina, D. G. Hopkinson, A. M. Rakowski, S. J. Magorrian, N. Clark, Y. M. Andreev, O. Kazakova, K. Novoselov, S. J. Haigh, V. I. Fal'ko, R. Gorbachev, 2D Materials **5**, 041009 (2018).
[11] D. A. Bandurin, A. V. Tyurnina, L. Y. Geliang, A. Mishchenko, V. Zolyomi, S. V. Morozov, R. K. Kumar, R. V. Gorbachev, Z. R. Kudrynskyi, S. Pezzini, Z. D. Kovalyuk, U. Zeilter, K. S. Novoselov, A. Patane, L. Eaves, I. I. Grigorieva, V. I. Fal'ko, A. K. Geim, Y. Cao, Nature Nanotech. **12**, 223 (2017).